C. R. Mecanique 347 (2019) 273–286

Contents lists available at ScienceDirect

Comptes Rendus Mecanique

www.sciencedirect.com

Patterns and dynamics: homage to Pierre Coullet / *Formes et dynamique : hommage à Pierre Coullet*

Advances in the analytical study of the dynamics of gaseous detonation waves

Paul Clavin

Aix–Marseille Université, CNRS, Centrale Marseille, IRPHE UMR7342, 49, rue Frédéric-Joliot-Curie, 13384 Marseille, France

ARTICLE INFO

Article history:
Received 29 November 2018
Accepted after revision 20 January 2019
Available online 28 March 2019

Keywords:
Nonlinear hyperbolic equations
Asymptotic analysis
Integral equation

ABSTRACT

Recent theoretical results on the dynamics of gaseous detonations are presented. An asymptotic analysis is performed, retaining the physical mechanisms controlling the modifications to the inner structure of the detonation. As a result, the system of hyperbolic equations for the compressible fluid mechanics coupled with a detailed chemical kinetics of heat release is reduced to a single integral equation for the propagation velocity of the combustion wave versus time. Concerning the direct initiation of spherical detonations by a blast wave, curvature effects are shown to be responsible for a critical condition of initiation. Near criticality, the role of the unsteadiness of the inner structure is pointed out. The whole complexity of the critical dynamics is reproduced and explained by the integral equation. The necessary background knowledge in gaseous detonation is recalled in the two first sections of the article in order to facilitate the reading by non-specialists.

1. Introduction

Detonations are supersonic combustion waves. Major advances in the understanding of the complex dynamics of these waves have resulted from asymptotic analyses that are reviewed in a 2017 article [1] and in a recent book [2], in which an history of the topic with an extensive list of references of the pioneering works can be found so that they are not included in the list of references of the present paper. In gaseous mixtures of fuels and oxygen, the propagation Mach number at ordinary conditions is in between 4 and 8. Detonations were discovered during the last quarter of the 19th century, half a century after the first experiments on premixed flames, which are subsonic waves (propagation Mach number $\approx 10^{-3}$–10^{-2}). A propagation velocity (a few km/s) of reaction waves in gaseous mixtures much faster than the mean velocity of molecules has been intriguing for a long time, even though shock waves were known to exist in inert gases. The steady inner structure of plane gaseous detonations was understood in 1940, more than half a century after the discovery of detonations. In the meantime, experiments showed the multidimensional geometry and the complex dynamics of the detonation fronts involving irregular and strongly unsteady cellular structures delimited by lines of singularities (triple points) propagating in the transverse direction. The explanation of the cellular structure has been elusive for a long time and the major steps in the understanding are recent. This is also the case for the initiation mechanism of a detonation by a blast wave. For example, the deflagration to detonation transition is not yet understood. The complex dynamics of detonation fronts is governed by the unsteadiness of their inner structure.

E-mail address: clavin@irphe.univ-mrs.fr.

https://doi.org/10.1016/j.crme.2019.03.008

The release of chemical heat results from the difference of binding energy of the molecules in the fresh mixture and in the combustion products, the latter being more stable than the former. Combustion proceeds through a complex chemical network of hundreds of elementary reactions involving tens of intermediate species with a wide range of timescales (10^{-3}–10^{-8} s). Two distinct periods are identified in the overall rate of heat release, an induction period in which the heat release is negligible, followed by an exothermic period. The induction delay is highly sensitive to temperature. There is no exothermic reaction in gaseous mixtures at atmospheric pressure for a temperature below 500 K (composition frozen far from chemical equilibrium). The induction delay varies from a few seconds at 800 K to less than 10^{-5} s at 1200 K. Above 1000 K, the duration of the exothermic period is of the same order of magnitude as the induction delay. The strong release of chemical energy induces nonlinear phenomena in the flow (as, for example, shock waves) retroacting upon the chemical kinetics controlling the overall rate of heat release.

The strategy developed at IRPHE to study such complex phenomena is the opposite of the most popular method based today on huge numerical codes including the whole details of the physical and chemical mechanisms characterized by a bunch of parameters. Instead, we consider limits of parameters for which the complexity of the basic system of conservation equations is reduced sufficiently to be solved analytically. The key point is to find out the relevant limits stressing the essential mechanisms governing the dynamics. The corresponding asymptotic analyses provide us with the physical insights that are necessary to put experiments and direct numerical simulations on a right track.

In the same spirit as in my conference at the 2017 meeting in Nice in honor of Pierre Coullet, this article is addressed to physicists who are not specialists of combustion theory and who are interested in nonlinear phenomena in fluid mechanics. The objective is neither to write another review article on detonations nor to present the details of the analyses. The purpose is to explain the phenomena in physical terms as they are enlightened by asymptotic analyses [3] and [4]. For simplicity, attention will be focused on one-dimensional problems describing the critical condition of the direct initiation process of detonation by local deposition of energy. The necessary background knowledge is recalled in the next section.

2. Physical mechanisms at work in gaseous detonations

2.1. Background

Consider a piston set in motion (subsonic velocity) at the closed end of an infinitely long tube in which an inert gas is enclosed. Soon after the piston reaches a constant subsonic velocity, a shock wave a few mean free paths thick is formed and propagates ahead of the piston in the quiescent gas at a constant and supersonic velocity. The flow velocity of the column of gas delimited by the piston and the shock has a uniform velocity equal to that of the piston. The length of this column increases linearly with time at a rate equal to the difference of propagation velocities between the supersonic shock and the subsonic piston. This self-similar solution in planar geometry is the result of the wave-breaking mechanism in compressible flows, described in one of the masterpieces of B. Riemann (1860). Conservation of mass, momentum, and total energy across the steady inner structure of the shock wave leads to the jump conditions of W.J.M. Rankine (1870) and P.H. Hugoniot (1889). Consider now a similar *Gedankenexperiment* for a reactive gaseous mixture. The increase of temperature across the shock ignites the chemical reaction and the chemical energy is released in the compressed gas after the induction delay. For a sufficiently large velocity of the piston, a reactive layer a few millimetres thick in the compressed gas stays attached to the inert shock. This piston-supported exothermic wave is called overdriven detonation. The separation of length scale between the lead shock in the inert gas and the reactive layer is a consequence of a well-known phenomenon in combustion pointed out by Ya. B. Zel'dovich and D.A. Frank-Kamenetskii (1938): the elementary reactions involved in the induction delay result from inelastic collisions that are less frequent than the elastic collisions controlling the inner structure of the lead shock. This is because the reactive collisions require a sufficiently high energy for breaking the molecules in the fresh mixture. The binding energy of the molecules is much larger than the thermal energy, explaining why the composition of a reactive mixture can stay frozen at ordinary initial conditions ($T \approx 300$ K, $p \approx 1$ atm). Even at high temperature ($T \approx 1000$–2500 K), the reactive collisions concerns the tail of the Maxwell–Boltzmann distribution. This leads to the Arrhenius law with a large activation energy $\mathcal{E}/k_{\mathrm{B}}T \gg 1$ describing the high thermal sensitivity and the thermal runaway that are responsible for the sudden and violent nature of some combustion phenomena. In simple words, as soon as the temperature is sufficiently high to initiate the exothermic reaction, the increase of temperature by the release of chemical heat further increases the reaction rate.

To summarise, the inner structure of a gaseous detonation consists in a (non-reactive) shock wave that can be considered as an hydrodynamic discontinuity, followed by a macroscopic reaction layer (induction + exothermic zone). In the laboratory frame, the velocity of the compressed gas is oriented in the direction of propagation. In the reference frame attached to the lead shock, the flow velocity is subsonic, of the order of the local speed of sound, and oriented in the opposite direction, see Fig. 1 in §4. This velocity is sufficiently large for neglecting heat conduction and viscosity (large Reynolds number, see below). The quasi-steady inner structure of a detonation is controlled by the balance between the reaction rate and the Lagrangian motion of fluid particles in the reference frame of the lead shock (balance between reaction and convection). Denoting a_{u} the sound speed in the initial mixture and t_{r}^{-1} the reaction rate at the compressed side of the lead shock (Neumann state), the detonation thickness is of order $d = a_{\mathrm{u}} t_{\mathrm{r}}$. The reaction rate being smaller than the collision frequency t_{coll}^{-1} (Arrhenius law: $t_{\mathrm{coll}}/t_{\mathrm{r}} \approx \mathrm{e}^{-\mathcal{E}/k_{\mathrm{B}}T} \ll 1$), the Reynolds number is large, $Re = a_{\mathrm{u}}^2 t_{\mathrm{r}}/\nu \gg 1$, where $\nu \approx a_{\mathrm{u}}^2 t_{\mathrm{coll}}$ is the molecular diffusion. Therefore, the dynamics of the inner structure is described by the reactive Euler equations for

inviscid compressible fluid complemented by the Rankine–Hugoniot conditions at the lead shock linking the conditions (pressure, temperature, and density) in the compressed gas just behind the shock (Neumann state) to the shock's velocity. The dynamics of the lead shock is a free boundary problem of an hyperbolic nature, which is closed by the conditions at the exit of the reaction zone.

Ten years after the discovery of the gaseous detonation, a young Russian scientist, V.A. Mikhel'son, reported in his 1893 PhD thesis at Moscow University that the conservation of mass, momentum, and total energy (including the binding energy of molecules) across the steady-state structure of a plane detonation wave leads to two families of solutions for a given supersonic propagation velocity. They differ by the velocity of the burnt gas relative to the shock wave, subsonic with a lead shock in one family and supersonic without lead shock in the other. The former is the solution mentioned above, while the latter is not relevant because ignition cannot occur at ordinary temperature. The two solutions merge at a minimum velocity of propagation $\mathcal{D}_{\rm CJ}$, for which the velocity of the burnt gas relative to the shock wave is sonic. There is no planar supersonic wave having a steady inner structure and propagating at a constant velocity $\mathcal{D}$ smaller than $\mathcal{D}_{\rm CJ}$, so that overdriven detonations are characterised by $\mathcal{D} > \mathcal{D}_{\rm CJ} \propto \sqrt{q_{\rm m}}$, $q_{\rm m}$ being the chemical energy per unit of mass of the reactive mixture. The marginal solution $\mathcal{D} = \mathcal{D}_{\rm CJ}$ is called the CJ solution in honor of the works of Chapman (1899) and Jouguet (1904) (it would have been better called Mikhel'son solution).

Moreover, CJ waves are self-sustained (propagating at constant velocity without the support of a piston). The sonic condition at the end of the reaction zone protects the inner structure of the detonation from being damped by the rarefaction wave. The latter develops systematically in the burnt gas between the flow at the exit of the reaction zone and the downstream boundary condition (zero velocity at the close end of a tube or at the centre for spherical detonations expanding freely in open space). The propagation velocity of overdriven detonations decreases down to $\mathcal{D}_{\rm CJ}$ under the influence of the rarefaction wave as soon as the supporting mechanism is suppressed.

2.2. The problem of direct initiation of detonation

The direct initiation process of detonation refers to the formation of a self-sustained detonation in open space in the decay of a strong blast wave produced by a concentrated energy source. The energy is deposited quasi-instantaneously in a hot spot of tinny size so that the density of energy is initially much larger than the density of chemical energy available in the gaseous mixture. Therefore, the initial condition corresponds to the Sedov (1946)–Taylor (1950) self-similar solution for a strong blast wave in an inert gas. Soon after, overdriven detonations are generated with a decreasing propagation velocity while the radius of the lead shock increases. The experiments show that a spherical CJ wave is formed at a finite distance $r_{\rm f}^*$ from the source only if the amount of energy liberated is sufficiently large $E > E^*$. A rough evaluation of this radius corresponds to $r_{\rm f}^* \approx (E^*/\rho_{\rm u} q_{\rm m})^{1/3}$ where $\rho_{\rm u}$ is the initial density of the reactive mixture. Initiation of detonation fails for $E < E^*$ and there is no spherical CJ detonation with a smaller radius. Pioneering numerical solutions were obtained around 1970 under the approximation considering the detonation wave as a discontinuity across which the planar jump conditions are satisfied. This approximation does not have a critical energy: in contrast with experiments, such a numerical solution predicts that the overdriven wave relaxes systematically to a CJ detonation, no matter how small the value of E is. This indicates that the critical condition for initiation is associated with the finite thickness of the detonation wave. A first criterion for the direct initiation was proposed by Zeldovich et al. (1956), assuming that the time taken for the blast wave velocity to decrease to $\mathcal{D}_{\rm CJ} \propto \sqrt{q_{\rm m}}$ must not be shorter than the reaction time. This criterion leads to a critical radius of the order of the thickness of the CJ wave and to a critical energy smaller than the experimental data by a factor 10^{-5} to 10^{-6} when relevant values of the reaction time are used,

$$\frac{E^*}{\rho_{\rm u} q_{\rm m}} = 2\frac{(\gamma+1)^4}{(\gamma-1)^2} d_{\rm o_{CJ}}^3, \qquad r_{\rm f}^* = 2^{1/3}\frac{(\gamma+1)^{4/3}}{(\gamma-1)^{2/3}} d_{\rm o_{CJ}} \approx 8\, d_{\rm o_{CJ}} \tag{1}$$

where $d_{\rm o_{CJ}}$ is the detonation thickness of the planar CJ wave and $\gamma \equiv c_p/c_v$ is the ratio of specific heat.

A further step was achieved forty years later by considering the small modification of the inner structure by the curvature of the wave [5]. This analysis of a curved CJ detonation was performed in the limit of a large activation energy $\mathcal{E}/k_{\rm B} \gg 1$, assuming that the inner structure is in steady state. Using a crude model for the inner structure of the plane CJ wave, namely the square-wave model for which the chemical energy is released instantaneously after the induction delay, this nonlinear analysis incorporates a small curvature term whose effect is amplified by the large activation energy. An extension of the analysis to a realistic inner structure is presented in § 6.2. The analysis in [5] leads to a non-linear relation between the propagation velocity of the curved CJ detonation $\mathcal{D}_{\rm CJ}$ and the curvature $d_{\rm o_{CJ}}/r_{\rm f}$, $r_{\rm f}$ denoting the radius of the lead shock. Denoting the CJ velocity of the plane wave $\mathcal{D}_{\rm o_{CJ}}$, the relation between $\mathcal{D}_{\rm CJ}/\mathcal{D}_{\rm o_{CJ}}$ and $r_{\rm f}/d_{\rm o_{CJ}}$ presents a turning point in the phase-space "propagation velocity–radius". There is no quasi-steady solution to spherical CJ waves below a critical radius $r_{\rm f}^*$, which is much larger than $d_{\rm o_{CJ}}$, essentially because of the large activation energy $\mathcal{E}/k_{\rm B}T \gg 1$. The critical radius $r_{\rm f}^*$ is typically 10^2–10^3 larger than that in (1). Therefore, the energy varying like r^3, the order of magnitude of E^* observed in experiments is recovered by the theoretical analysis [5]. The numerical simulations of He [6] using a detailed chemical scheme for the combustion of hydrogen–oxygen mixtures showed results in satisfactory agreement with the theoretical prediction, even though unsteady effects that are neglected in [5] are non-negligible in the numerical simulation. The

importance of unsteadiness in the direct initiation process of gaseous detonation was also observed later in numerical simulations using a simple one-step exothermal reaction governed by an Arrhenius law [7]. The unsteady terms are found to be even larger than the geometrical terms describing the curvature effect. However, surprisingly, the critical radius was not much different from that predicted in [5], the ratio of the numerical radius to the theoretical radius being between 2 and 4. Considering the difference of models of inner structure in [5] and in [7], the agreement is quite satisfactory indeed.

The purpose of the analytical study [4] is precisely to investigate the role of unsteadiness in direct initiation of detonation, especially near the critical radius. An overview of the asymptotic method and of the results are presented in § 5 and § 6. A first step consists in analyzing the decay to the CJ regime in planar geometry when the supporting piston is suddenly arrested. This hyperbolic problem is old and has been solved under the approximation of a detonation considered as a discontinuity (detonation front without modification of the inner structure) following Chandrasekhar (1943) and Friedrichs (1948) for the decay of a pure shock wave. The analytical solution taking into account the unsteadiness of the inner structure of the detonation has been obtained only recently [3] and is presented in § 5.2.

The mathematical formulation is given in § 3. Physical insights are presented in § 4 followed by the analyses of the detonation decay in the planar and spherical geometry in § 5 and § 6.

3. General formulation

3.1. Constitutive equations

In spherical geometry, $\nabla\cdot\mathbf{u} = \partial u/\partial r + 2u/r$, the reactive Euler's equations are

$$\frac{1}{\rho}\left(\frac{\partial}{\partial t} + u\frac{\partial}{\partial r}\right)\rho + \frac{\partial u}{\partial r} + 2\frac{u}{r} = 0, \qquad \rho\left(\frac{\partial}{\partial t} + u\frac{\partial}{\partial r}\right)u = -\frac{\partial p}{\partial r} \tag{2}$$

$$\left(\frac{\partial}{\partial t} + u\frac{\partial}{\partial r}\right)\left[\ln T - \frac{(\gamma-1)}{\gamma}\ln p\right] = \frac{q_{\rm m}}{c_p T}\frac{\dot w(Y,T,p)}{t_{\rm r}}, \quad \left(\frac{\partial}{\partial t} + u\frac{\partial}{\partial r}\right)Y = \frac{\dot w(Y,T,p)}{t_{\rm r}} \tag{3}$$

where ρ, p and u are respectively the density, the pressure, and the radial velocity in the laboratory frame and γ, $q_{\rm m}$, T, Y, $t_{\rm r}$ and $\dot w \geqslant 0$ are respectively the ratio of specific heat $\gamma \equiv c_p/c_v$ = cst., the chemical heat release per unit mass of mixture, the temperature, the progress variable ($Y = 0$ in the initial mixture and $Y = 1$ in the burned gas), the reaction time at the Neumann state of the CJ wave and the non-dimensional heat-release rate expressed in term of the thermodynamic variables. The first equation in (3) is the conservation of energy written in the entropy form. The entropy production results from the rate of heat release, heat conduction and molecular diffusion being negligible behind the lead shock. The second equation in (3) is a short notation for a complex chemical kinetics of combustion. The pressure p and the sound speed a are given by the ideal gas law

$$p = \frac{\gamma-1}{\gamma}c_p\rho T, \qquad a = \sqrt{\gamma\,\frac{p}{\rho}} \tag{4}$$

Using the mass conservation in (2) and the equation of state in (4) for eliminating ρ and T, the energy equation in (3) can be written in terms of p and u in the form

$$\frac{1}{\gamma p}\left(\frac{\partial}{\partial t} + u\frac{\partial}{\partial r}\right)p + \frac{\partial u}{\partial r} + 2\frac{u}{r} = \frac{q_{\rm m}}{c_p T}\frac{\dot w}{t_{\rm r}} \tag{5}$$

Equations for the conservation of mass and momentum in (2) can be put in the form of two hyperbolic equations for u and p when the equation for conservation of momentum in (2) multiplied by $a/(\gamma p) = 1/(\rho a)$ is added to or subtracted from (5)

$$\frac{1}{\gamma p}\left[\frac{\partial}{\partial t} + (u\pm a)\frac{\partial}{\partial r}\right]p \pm \frac{1}{a}\left[\frac{\partial}{\partial t} + (u\pm a)\frac{\partial}{\partial r}\right]u = \frac{q_{\rm m}}{c_p T}\frac{\dot w}{t_{\rm r}} - 2\frac{u}{r} \tag{6}$$

When (4) is used and when the expression of the reaction rate in term of the thermodynamic variables $\dot w(T,p,Y)$ is known, equations (3) and (6) form a closed set for p, u, T, and Y. Equations (3) describe the entropy wave propagating with the velocity of the flow. Equation (6) is the extension of the usual characteristic equations to the case of a reacting gaseous mixture in spherical geometry. They describe compressible waves $\mathcal{C}_+$ and $\mathcal{C}_-$ propagating in two opposite directions at the speed of sound relatively to the fluid particles. When the right-hand side is set equal to zero, the linearized version of (6) represents the simple waves of planar acoustics $\delta p = \pm\rho a\delta u$. The divergence of the spherical flow $2u/r$ in the right-hand side of (6) is the only difference with the planar geometry.

3.2. Boundary conditions

Introducing the instantaneous radius and velocity of the shock front $r = r_f(t)$, $\mathcal{D}(t) \equiv \mathrm{d}r_f/\mathrm{d}t > 0$, it is convenient to consider the coordinate attached to the lead shock

$$x \equiv r - r_f(t) \quad \Rightarrow \quad \partial/\partial r \to \partial/\partial x, \quad \partial/\partial t \to \partial/\partial t - \mathcal{D}(t)\partial/\partial x \tag{7}$$

For an expanding spherical detonation, $\mathrm{d}r_f/\mathrm{d}t > 0$, $u \geqslant 0$, the initial mixture and the compressed gas correspond to $x > 0$ and $x \leqslant 0$ respectively. The boundary conditions at the compressed gas side $x = 0^-$ of the shock front (called Neumann state and denoted by the subscript N) take the form

$$x = 0^- : \quad Y = 0, \quad \dot{w} = \dot{w}_N(T_N) > 0, \quad p = p_N(t), \quad T = T_N(t), \quad u = u_N(t) \tag{8}$$

where, using the Rankine–Hugoniot conditions, $p_N(t)$, $T_N(t)$, and $u_N(t)$ are expressed in term of $\mathcal{D}(t)$ and the thermodynamic variables p_u and T_u of the quiescent mixture, frozen in the initial state denoted by the subscript u. The propagation velocity $\mathcal{D}(t)$ is determined when a rear boundary condition at the exit of the reaction zone is applied to the solution to the hyperbolic equations (3) and (6) satisfying (8). The rear boundary condition of a weakly curved detonation $r_f/a_N t_r \gg 1$ takes a simple form if the length scale of the external flow in the burnt gas $u_{ext}(r,t)$ (rarefaction wave) is larger than the detonation thickness, $l_{ext} \gg a_N t_r$, $1/l_{ext} \equiv |(1/u_{ext})\partial u_{ext}/\partial r|_{r=r_f(t)}$. Then, introducing the non-dimensional coordinate ξ attached to the moving front of the lead shock (radius r_f),

$$\xi \equiv \frac{x}{a_u t_r} = \frac{r - r_f(t)}{a_u t_r} \tag{9}$$

and denoting the end of the reaction by a subscript b ($\xi = \xi_b < 0$)

$$|\xi_b| = O(1), \qquad \xi \leqslant \xi_b : \ \dot{w}(Y = 1, T) = 0, \qquad \xi_b < \xi \leqslant 0 : \ \dot{w}(Y, T) > 0 \tag{10}$$

the rear boundary condition of the inner structure takes the form

$$\xi = \xi_b < 0 : \ u = u_b(t), \quad u_b(t) = u_{ext}(r_f(t), t) \tag{11}$$

where the flow field of burnt gas $u_{ext}(r,t)$ is solution to an external problem (inert rarefaction wave). The solution to (3) and (6) satisfying (8) and (11) yields the expression of $\mathcal{D}(t)$ as a functional of $u_b(t)$.

Analytical solutions to the decay to the CJ regime cannot be obtained without further simplification. Not only the intrinsic dynamics of the inner structure is a tough problem, but also the external flow $u_{ext}(r,t)$ is a rarefaction wave that depends on the dynamics of its leading edge so that the boundary condition $u_b(t)$ in (11) depends in fact on the solution. This difficulty is overcome in § 6.1 thanks to the quasi-transonic character of the flow at the exit of the exothermic zone when approaching the CJ regime. The dynamics of the inner structure is solved in § 5.

4. Physical insights

The purpose of this section is to identify the main physical mechanisms controlling the dynamics in order to determine the limit of parameters to be used in the asymptotic analysis. From now on, we consider the reference frame attached to the lead shock of a detonation propagating with a positive velocity $\mathcal{D} > u > 0$. The flow velocity in the inner structure of a detonation is subsonic relatively to the shock and its absolute value increases $0 < (\mathcal{D} - u) < a$ with the amount of released heat from the Neumann state at $x = 0^-$ to the end of the reaction at $x = x_b < 0$, $(\mathcal{D} - u_N) < (\mathcal{D} - u_b)$, see Fig. 1. The sonic condition is verified only at the exit of the reaction zone of the CJ wave, $(\mathcal{D}_{CJ} - u_b) = a_b$ while $(\mathcal{D} - u_b) < a_b$ in the overdriven regimes.

4.1. Newtonian approximation

Across the inner structure of usual gaseous detonations, adiabatic compressional heating is not important. Its effect on temperature is relatively small compared to the temperature increase due to the release of chemical heat. Therefore, the pressure term can be neglected in Eqs. (3) governing the downstream running entropy wave,

$$\left(\frac{\partial}{\partial t} + (u - \mathcal{D})\frac{\partial}{\partial x}\right) T \approx \frac{q_m}{c_p}\frac{\dot{w}(T,Y)}{t_r}, \quad \left(\frac{\partial}{\partial t} + (u - \mathcal{D})\frac{\partial}{\partial x}\right) Y = \frac{\dot{w}(T,Y)}{t_r} \tag{12}$$

$$x = 0^- : \qquad T = T_N(t), \quad Y = 0 \tag{13}$$

This corresponds to what is called the Newtonian approximation $0 < (\gamma - 1) \ll 1$. The compressible phenomena are fully retained in the Rankine–Hugoniot conditions at the lead shock and also in the characteristic equations (6) of the compressible modes propagating in the two directions across the inner structure of the detonation, see Fig. 1. For usual gaseous

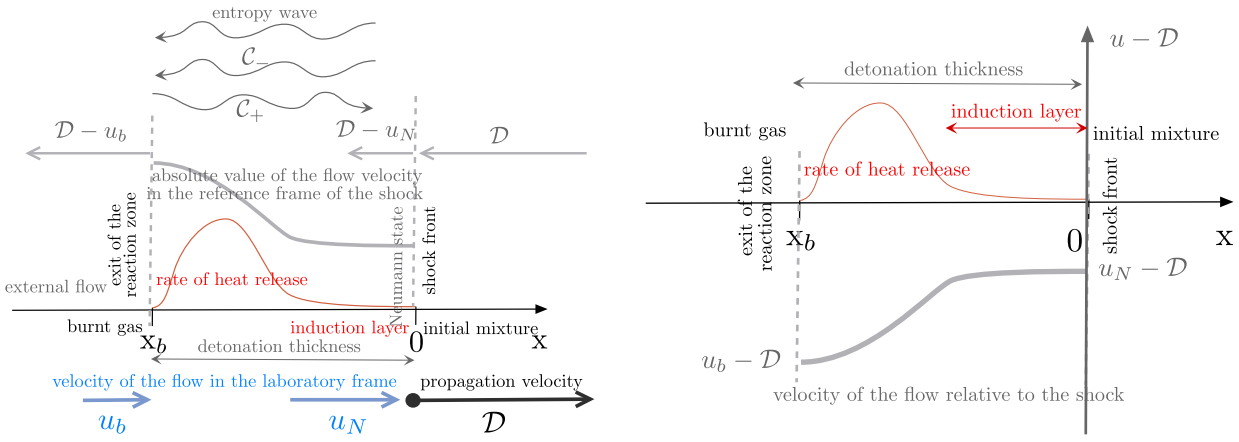

Fig. 1. Sketch of the inner structure of a gaseous detonation. Left: the profile of the rate of heat release is plotted with the absolute value of the flow velocity in the reference frame of the lead shock, $(\mathcal{D}-u)>0$. The latter has a shape similar to that of the temperature distribution. The upstream and downstream running modes (compressible simple waves), respectively $\mathcal{C}_+$ and $\mathcal{C}_-$, are shown on top, upstream, and downstream, referring to the flow in the reference frame of the lead shock. The downstream running entropy wave that propagates with the fluid particles at the flow's velocity is also shown. Right: plot of the flow velocity in the reference frame attached to the lead shock, $(u-\mathcal{D})<0$. Its profile is similar to that of the reduced flow field $\mu(\xi,\tau)>0$ used in the asymptotic analysis, $\mu\in[\mu_b,\,1]$, $0<\mu_b\ll 1$, see definition (23).

detonations, the activation energy is large and the variation of the reaction rate with the pressure can be neglected in front of its variation with temperature and with the progress variable, $\dot{w}(T,Y)$.

The solution to (12)–(13) is easily obtained if the variation of $(u-\mathcal{D})$ with time is negligible. Introducing the delay associated with a fluid particle issued from the lead shock to reach the point at a distance $|x|$ from the shock, $\Delta(x)=\int_x^0 \mathrm{d}x'/(\mathcal{D}-u)>0$, the instantaneous distribution of the rate of heat release $w(x,t)=\dot{w}(T,Y)$ obtained from (12)–(13) then takes the form

$$w(x,t)=\overline{w}\Big(x,\,T_{\mathrm{N}}\big(t-\Delta(x)\big)\Big) \tag{14}$$

where $\overline{w}(x,T_{\mathrm{N}})$ is the steady-state solution associated with the boundary condition $x=0:\ T=T_{\mathrm{N}},\,Y=0$. Equation (14) means that the value of the instantaneous distribution of the reaction rate $w(x,t)$ at a distance $|x|$ from the lead shock is related to its value in the steady state, corresponding to a Neumann condition defined at a time shifted in the past by the delay $\Delta(x)$. The temperature $T_{\mathrm{N}}(t)$ at the Neumann state is related to the propagation velocity of the lead shock $\mathcal{D}(t)$ through the Rankine–Hugoniot conditions, so that the distribution of the rate of heat release (14) is expressed in terms of the propagation velocity at an early time. Solving (6) with the boundary conditions (8) and (11) is still a too complicated hyperbolic problem for a general analytical solution $\mathcal{D}(t)$ to be obtained.

4.2. Two timescales in the feedback loops

According to the Rankine–Hugoniot conditions, the variation of the propagation velocity $\mathcal{D}(t)$ generates perturbations of p and u at the Neumann state. They are transported toward the reacting gas by the entropy wave with the absolute velocity $(\mathcal{D}-u)>0$ and also by the downstream running characteristics $\mathcal{C}_-$ with the absolute velocity $a+(\mathcal{D}-u)>a$. Part of the resulting disturbances of the source terms in the right-hand side of (6) are sent back to the shock by the upstream running mode $\mathcal{C}_+$ propagating with the velocity $a-(\mathcal{D}-u)>0$, see Fig. 1. When these upstream running disturbances reach the Neumann state, they modify $\mathcal{D}(t)$ through the Rankine–Hugoniot conditions. Therefore the instantaneous propagation velocity of the lead shock, $\mathcal{D}(t)$ is determined by the cumulative effects of a continuous set of feedback loops, illustrating the complexity of the hyperbolic problem. For a fixed condition at the exit of the reaction zone, these loops can lead to an intrinsic instability of the inner structure studied by asymptotic analyses in [3,8] and [9], briefly recalled in planar geometry in §5.2.

If the subsonic velocity of the flow $\mathcal{D}-u$, $a>(\mathcal{D}-u)>0$, is sufficiently close to the speed of sound (quasi-transonic flow), $0<[a-(\mathcal{D}-u)]\ll a$, the problem of the dynamics of the inner structure is one of two timescales since the propagation velocity of the downstream running modes (entropy wave and characteristics $\mathcal{C}_-$) becomes much larger than that of the upstream running mode $\mathcal{C}_+$, $(\mathcal{D}-u)\gg[a-(\mathcal{D}-u)]$ and $a+(\mathcal{D}-u)\gg[a-(\mathcal{D}-u)]$. Therefore, the transit time of the disturbances that are propagated by the downstream running modes is much shorter than those propagated by $\mathcal{C}_+$. The delay in each feedback loop is controlled by the slowest mode, namely $\mathcal{C}_+$, the effect of the downstream running modes being quasi-instantaneous. Therefore the characteristic time of the overall dynamics of the inner structure is larger than the transit time of a fluid particle across the detonation thickness and, to leading order in a two timescales analysis, the delay Δ can be neglected in (14),

$$[a-(\mathcal{D}-u)]\ll a \quad \Rightarrow \quad w(x,t)\approx \overline{w}(x,T_{\rm N}(t)) \tag{15}$$

Equation (15) is valid for any complex chemical scheme. Moreover, the effects of small variations of $T_{\rm N}(t)$ in (15) are amplified by a high thermal sensitivity.

Unfortunately, the quasi-transonic approximation $[a-(\mathcal{D}-u)]\ll a$ is not uniformly valid in the inner structure of real gaseous detonations, even for overdriven regimes close to the CJ regime, $(\mathcal{D}-u_{\rm b})\approx a_{\rm b}$. In the induction layer, one has typically $\mathcal{D}-u_{\rm N}=0.3\,a_{\rm N}$. The quasi-transonic approximation is verified everywhere in the inner structure of detonations close to the CJ regime only in the limit of small heat release. This limit provides the framework for a systematic theoretical analysis of the unsteady inner structure of detonations. Even though the limit of small heat release is not realistic for real detonations, it is a convenient approximation provided that the lead shock is still considered as a discontinuity. All the mechanisms involved in the dynamics of the inner structure are well kept and the technical difficulty associated with the variation of the sound speed that does not play a significant role is suppressed. This yields analytical results that are qualitatively relevant and quantitative agreement with real detonations can be obtained simply by rescaling the asymptotic results, see the end of §5.2.

5. Asymptotic analysis of the unsteady inner structure

The analyses presented below were carried out in the limit of small heat release $\epsilon^2\equiv q_{\rm m}/c_pT_{\rm u}\ll 1$, using the Newtonian approximation (γ close to unity) in order to suppress the compressional heating,

$$\epsilon\equiv(M_{\rm o_{CJ}}-1)\ll 1, \qquad (\gamma-1)/\epsilon\ll 1 \tag{16}$$

where $M_{\rm o_{CJ}}\equiv \mathcal{D}_{\rm o_{CJ}}/a_u\approx 1+\sqrt{q_{\rm m}/c_pT_{\rm u}}$ is the Mach number of the planar CJ wave in steady state propagating at the velocity $\mathcal{D}_{\rm o_{CJ}}$, $a_{\rm u}$ being the speed of sound in the initial mixture. A sufficiently large thermal sensitivity then ensures that the small fluctuations that are produced in the limit (16) produce a substantial effect on the overall dynamics, $\delta\mathcal{D}(t)/\mathcal{D}=O(1)$.

5.1. Formulation in the asymptotic limit

On the basis of the results of [5], anticipating that the critical radius of the lead shock is larger than the detonation thickness, a non-dimensional curvature $\kappa(\tau)$ of order unity in the limit (16) is introduced by

$$\frac{a_{\rm u}t_{\rm r}}{r_{\rm f}(\tau)}=\epsilon\kappa(\tau), \qquad \kappa=O(1) \tag{17}$$

For conditions close to the CJ regime of plane detonations we introduce the following dimensionless quantities of order unity in the limit (16), $\mu(\xi,\tau)$, $\pi(\xi,\tau)$ and $\dot\alpha_\tau(\tau)$ for, respectively, the flow velocity relative to the lead shock, the pressure, and the instantaneous propagation velocity of the lead shock $\mathcal{D}(t)={\rm d}r_{\rm f}/{\rm d}t$,

$$\frac{u-\mathcal{D}_{\rm o_{CJ}}}{a_{\rm u}}\equiv -1+\epsilon\,\mu(\xi,\tau), \quad \frac{\mathcal{D}-\mathcal{D}_{\rm o_{CJ}}}{a_{\rm u}}\equiv\epsilon\,\dot\alpha_\tau(\tau), \quad \frac{1}{\gamma}\ln\left(\frac{p}{p_{\rm u}}\right)\equiv\epsilon\,\pi(\xi,\tau) \tag{18}$$

where τ is the reduced time of order unity describing the dynamics, see (25) below. The objective of this subsection is to show that, in the limit (16), the non-dimensional shock velocity $\dot\alpha_\tau(\tau)$ is obtained by solving a single (nonlinear) partial–differential equation for the non-dimensional flow field $\mu(\xi,\tau)$,

$$\frac{\partial\mu}{\partial\tau}+[\mu-\dot\alpha_\tau(\tau)]\frac{\partial\mu}{\partial\xi}=\frac{w(\xi,\tau)}{2}-(1+\mu)\kappa(\tau) \tag{19}$$

$$\xi=0:\mu=1+2\dot\alpha_\tau(\tau), \qquad \xi=\xi_{\rm b}(\tau):\mu=\mu_{\rm b}(\tau) \tag{20}$$

where $\mu_{\rm b}(\tau)$ is a given function obtained from the external flow in the burnt gas.

In the limit of small heat release (16), the speed of sound $a/a_{\rm u}=\sqrt{T/T_{\rm u}}$ and the curvature term $r_{\rm f}/r$ are, according to (9) and (17), almost constant across the inner structure of the detonations $\xi=O(1)$, $a/a_{\rm u}=1+O(\epsilon)$, $r_{\rm f}/r=1/[1+\epsilon\kappa\xi]$. When these terms, which are of order smaller than ϵ^2, are neglected, Eqs. (6), written in the reference frame attached to the lead shock (7), using the notations (9) and (18), take the non-dimensional form

$$\epsilon\left[t_{\rm r}\frac{\partial}{\partial t}+[-2+\epsilon(\mu-\dot\alpha_\tau)]\frac{\partial}{\partial\xi}\right](\pi-\mu)=\epsilon^2\dot w-2\epsilon^2(1+\mu)\kappa \tag{21}$$

$$\epsilon\left[t_{\rm r}\frac{\partial}{\partial t}+\epsilon(\mu-\dot\alpha_\tau)\frac{\partial}{\partial\xi}\right](\pi+\mu)=\epsilon^2\dot w-2\epsilon^2(1+\mu)\kappa \tag{22}$$

obtained by using (16)–(18) in the form

$$\frac{u}{a_{\rm u}}=\epsilon(1+\mu), \quad \frac{(u-\mathcal{D})}{a_{\rm u}}=\epsilon(\mu-\dot\alpha_\tau)-1, \quad \frac{u}{r}=\epsilon^2\kappa(1+\mu)\frac{r_{\rm f}}{r} \tag{23}$$

Using the Rankine–Hugoniot relations, the boundary conditions at the Neumann state take the form,

$$\xi = 0 : \mu = \mu_{\rm N}(\tau) = (1 + 2\dot{\alpha}_\tau) + O(\epsilon), \quad \pi = \pi_{\rm N}(\tau) = 2(1 + \dot{\alpha}_\tau) + O(\epsilon) \tag{24}$$

The two-timescale nature of the dynamics in the limit (16) is revealed by the comparison of (21) and (22). The velocity of the simple wave (21), issued from the lead shock ($\xi = 0$) and propagating toward the exit of the reaction zone (in the negative ξ direction) is larger (by a factor of $1/\epsilon$) than the velocity of the simple wave (22) propagating in the opposite direction for closing the feedback loops. Therefore, to leading order in the limit (16), the propagation mechanism in (21) is instantaneous and the dynamics of the inner structure is controlled by the simple wave (22). The resulting dynamics is slow at the scale of the transit time $t_{\rm r}$ of a fluid particle propagating from the lead shock up to the end of the reaction zone. Therefore, the reduced timescale τ of order unity is

$$\tau \equiv \epsilon \frac{t}{t_{\rm r}}, \qquad \frac{\partial}{\partial t} = \frac{\epsilon}{t_{\rm r}} \frac{\partial}{\partial \tau} \tag{25}$$

The leading order of (21), $\partial(\pi - \mu)/\partial\xi = 0$, shows using (24) that the quantity $\pi - \mu$ is constant, $(\pi - \mu) \approx 1$. Expressed in terms of the reduced time (25), the leading order of (22) in the limit $\epsilon \ll 1$, after division of the two sides by ϵ^2, takes the form (19). Skipping for the moment the matching difficulty mentioned at the end of § 3.2, the function $\mu_{\rm b}(\tau)$ is given by the external solution in the burnt gas, except for the CJ regime, for which the dynamics of the inner structure is decoupled from the flow of burnt gas by the sonic condition,

$$\text{CJ wave:} \qquad \mu_{\rm b}(\tau) = \dot{\alpha}_\tau(\tau) \tag{26}$$

($\dot{\alpha}_\tau = 0$ in the planar CJ wave, $\kappa = 0$).

The unsteady distribution of the reaction rate (15) requires to compute the inner structure of a family of steady overdriven detonations $\overline{w}(x, \overline{T}_{\rm N})$ for different propagation velocity $\overline{\mathcal{D}}$, $\mathcal{D}$, and $T_{\rm N}$, being in one-to-one correspondence (Rankine–Hugoniot relation). Numerical simulations of overdriven detonations of hydrogen–oxygen mixtures [10] show that $\overline{w}(x, \overline{T}_{\rm N})$ can be well approximated from the distribution of the CJ detonation in the steady state, $w_{\rm o_{CJ}}(\xi) \geqslant 0$ by rescaling the length scale with the time-dependent induction length, yielding

$$w(\xi, \tau) = {\rm e}^{b\dot{\alpha}_\tau(\tau)} w_{\rm o_{CJ}}(\xi\, {\rm e}^{b\dot{\alpha}_\tau(\tau)}), \quad \text{with} \quad \int_{-\infty}^{0} w_{\rm o_{CJ}}(\xi){\rm d}\xi = 1 \;\Rightarrow\; \int_{-\infty}^{0} w(\xi, \tau){\rm d}\xi = 1 \tag{27}$$

where the parameter b characterizes thermal sensitivity,

$$b = 2(\gamma - 1)\epsilon \frac{\mathcal{E}}{k_{\rm B} T_u} \tag{28}$$

and $\mathcal{E}$ is the activation energy of the Arrhenius law controlling the variation of the induction length with the Neumann temperature. The normalization condition in (27) corresponds to a reference timescale $t_{\rm r}$ in (3)–(9) equal to the reaction time at the Neumann state of the CJ wave, so that its non-dimensional thickness is equal to unity, $\xi \leqslant -1 : w_{\rm o_{CJ}}(\xi) = 0$, $-1 < \xi \leqslant 0 : w_{\rm o_{CJ}}(\xi) > 0$. Therefore, the end of the reaction zone in the unsteady structure is located at

$$\xi = \xi_{\rm b}(\tau) = -{\rm e}^{-b\dot{\alpha}_\tau(\tau)}, \qquad \xi \leqslant \xi_{\rm b}(\tau) : w(\xi, \tau) = 0 \tag{29}$$

To summarize, when (27) is inserted into (19), the hyperbolic problem (2)–(11) is reduced in the asymptotic limit (16) to solve (19) with the boundary conditions (20) for $\xi_{\rm b}$ in (29). If the flow of shocked gas is kept subsonic relatively to the lead shock, as is the case in the steady state, the term in the bracket on the left-hand side of (19), computed from (18),

$$\xi_{\rm b} < \xi \leqslant 0 : \quad [\mu - \dot{\alpha}_\tau] = [a_{\rm u} - (\mathcal{D} - u)]/\epsilon a_{\rm u} > 0 \tag{30}$$

is positive everywhere across the inner structure and increases from the end of the heat release ($\xi = \xi_{\rm b} < 0$) to the lead shock ($\xi = 0$), like the flow velocity u increases in the laboratory frame from $u_{\rm b}$ to $u_{\rm N}$ under the effect of the chemical heat release, see Fig. 1 (right). Therefore, the wave-breaking mechanism by the nonlinear term $(\mu - \dot{\alpha}_\tau)\partial\mu/\partial\xi$ cannot be produced in the reacting flow behind the lead shock.

5.2. Dynamics of planar detonations

The solution to (19)–(20) with (29) leads to an integral equation for the instantaneous propagation velocity $\dot{\alpha}_\tau(\tau)$. Before considering the direct initiation of detonations, the dynamics of planar detonations is worth recalling. The equation to be solved is (19) for $\kappa = 0$ and the stability of planar detonations against planar disturbances is performed for a constant value of the flow velocity at the end of the exothermic reaction, $\mu_{\rm b} = \overline{\mu}_{\rm b} = $ cst. in (20). For any positive value $\overline{\mu}_{\rm b} > 0$, there are two steady-state solutions, only one describing a (weakly) overdriven wave, $[\overline{\mu}(\xi, \overline{\mu}_{\rm b}) - \dot{\overline{\alpha}}_\tau(\overline{\mu}_{\rm b})] > 0$, $\dot{\overline{\alpha}}_\tau(\overline{\mu}_{\rm b}) > 0$,

$$\overline{y}/b = (1+\overline{\mu}_b)^{-1}\overline{\mu}_b^2/2, \qquad \overline{\mu}(\xi,\overline{y}) - \overline{y}/b = \sqrt{(\overline{\mu}_b - \overline{y}/b)^2 + \mu_{o_{CJ}}^2(\xi\, e^{\overline{y}})} \tag{31}$$

where the notation $y \equiv b\dot{\alpha}_\tau$ has been used and where the marginal CJ solution $\mu_{o_{CJ}}(\xi)$ ($\overline{\mu}_b = 0$, $\overline{y} = 0$) is a increasing function from 0 at the end of the reaction $\xi = -1$ to 1 at the Neumann state $\xi = 0$. The linear version to the hyperbolic equation (19) is solved in [3] and [8] for a parameter b of order unity in the limit (16), corresponding to a large activation energy, $\mathcal{E}/k_B T_u \gg 1$. Introducing the decomposition $y(\tau) = \overline{y} + \delta y(\tau)$, the variation of the shock velocity $\delta y(\tau)$ is found to be solution to an integral equation,

$$b = O(1), \quad \kappa = 0: \quad 2(1+2\overline{y}/b)\,\delta y(\tau) = \int_{-\infty}^{0} g(\xi)\, y(\tau + \overline{\zeta}(\xi))\,d\xi \tag{32}$$

$$\text{where} \quad g(\xi) \equiv \left\{ \frac{b}{2}\frac{\partial}{\partial y}\left[e^y w_{o_{CJ}}(\xi\, e^y)\right]_{y=\overline{y}} + \frac{d\overline{\mu}}{d\xi} \right\}, \quad \overline{\zeta}(\xi) \equiv -\int_{\xi}^{0} \frac{d\xi'}{\overline{\mu}(\xi')} < 0, \quad \overline{\zeta}_b \equiv -\int_{\overline{\xi}_b = -e^{-\overline{y}}}^{0} \frac{d\xi'}{\overline{\mu}(\xi')} \tag{33}$$

where $|\overline{\zeta}_b| < \infty$ is the total transit time of the perturbation transported upstream by the compressible mode $\mathcal{C}_+$ to reach the lead shock from the end of the reaction and $|\overline{\zeta}(\xi)| < |\overline{\zeta}_b|$ is the transit time from the position ξ. The physical interpretation of (32) is straightforward: the function $g(\xi)\, y(\tau - |\overline{\zeta}|)$ is the perturbation of the shock velocity at time τ resulting from the local modification at ξ of the reaction rate produced at earlier time by the downstream propagating modes (entropy wave and $\mathcal{C}_-$), the time lag $|\overline{\zeta}(\xi)|$ being the delay taken by $\mathcal{C}_+$ for sending the perturbation back to the lead shock. The integral term in (32) corresponds to the cumulative effects of the loops associated with all the points in the internal structure. The lower bound of the integral in (32) is replaced by $-\infty$ because the kernel $g(\xi)$ vanishes for $\xi < \overline{\xi}_b$. The stability limit is obtained by looking for a solution to (32) in the form $\delta y(\tau) = e^{\sigma\tau}$ yielding a transcendental equation for the linear growth rate σ (a complex number) corresponding to the Laplace transform of g,

$$\int_{-\infty}^{0} \tilde{g}(\overline{\zeta})\, e^{\sigma\overline{\zeta}}\, d\overline{\zeta} = 2(1+2\overline{y}/b) \quad \text{where} \quad \tilde{g}(\overline{\zeta}) \equiv \mu_{o_{CJ}}(\xi(\overline{\zeta}))\, g(\xi(\overline{\zeta})) \tag{34}$$

the function $\xi(\overline{\zeta})$ being obtained by inversion of (33), corresponding to a one-to-one relation between ξ and ζ. Equation (34) has a discrete set of complex roots σ_i, $i = 1, 2\ldots$. For a temperature sensitivity sufficiently small and for a distribution $w_{o_{CJ}}(\xi)$ sufficiently smooth, the detonation is stable against planar disturbances; the real part of all the roots is negative, corresponding to damped oscillatory modes (Im $\sigma_i \neq 0$, Re $\sigma_i < 0$ $\forall i$). An oscillatory instability occurs when b is slightly increased above the instability threshold b_c at which one of the oscillatory modes σ_j becomes neutral, $b = b_c$: Re $\sigma_j = 0$, Im $\sigma_j \neq 0$ of order unity, $b > b_c$: Re $\sigma_j > 0$. When b is further increased, many unstable oscillatory modes develop. The value b_c depends on the shape of $w_{o_{CJ}}(\xi)$. For typical distributions $w_{o_{CJ}}(\xi)$ of real detonations, the parameter b_c at the instability threshold and the reduced frequency of the marginal mode are of order unity. The stiffer is $\overline{w}_{o_{CJ}}(\xi)$ the smaller is b_c and the larger is the frequency.

A nonlinear extension to marginally unstable detonation in planar geometry has also been obtained [3]

$$2\,y(\tau) = \overline{y} + \int_{-\infty}^{0} G\Big(\xi,\, y(\tau + \overline{\zeta}(\xi))\Big)\,d\xi, \qquad G(\xi,y) \equiv W(\xi,y) + \frac{d\mu_{o_{CJ}}}{d\xi}\, y \tag{35}$$

$$\text{where} \quad W(\xi,y) \equiv \frac{b}{2}\left[e^y w_{o_{CJ}}(\xi e^y) - w_{o_{CJ}}(\xi)\right], \quad \int_{-\infty}^{0} W(\xi,y)\,d\xi = 0, \quad \int_{-\infty}^{0} G(\xi,y)\,d\xi = y \tag{36}$$

and $2\overline{y}/b$ has been neglected in front to 1 in the boundary condition at $\xi = 0$. The numerical solution to (35) shows a supercritical bifurcation. Nonlinear oscillations develops for b slightly larger than b_c, followed by a transition to a chaotic signal $y(\tau)$ through period doubling when b is further increased.

The delay $|\zeta_b|$ increases when approaching the CJ regime ($\overline{\mu}_b \to 0^+$) and, for an usual reaction rate, it diverges at CJ. This does not change the stability analysis, because $\tilde{g}(\zeta)$ decreases sufficiently quickly to zero when ζ increases. In that respect, the marginal character of the CJ regime does not play a particular role. This is not the case for the linear response to disturbances of the flow at the exit of the reaction zone $\delta\mu_b(\tau)$. For a slightly overdriven detonation $\overline{\mu}_b > 0$ in the stable domain $b < b_c$, $|\delta\mu_b| < \overline{\mu}_b$, one gets

$$2\delta\dot{\alpha}_\tau(\tau) = \int_{-\infty}^{0} g(\xi)\,\delta\dot{\alpha}_\tau(\tau + \overline{\zeta}(\xi))\,d\xi + \overline{\mu}_b\,\delta\mu_b(\tau - |\overline{\zeta}_b|) \tag{37}$$

When the timescale of the forcing term $\delta\mu_b(\tau)$ is larger than that of the inner response, the time delays can be forgotten, leading to a quasi-steady response. The linear response (37) has no meaning for a CJ wave since $\overline{\mu}_b = 0$. The relevant problem is to determine the decay of the propagation velocity of a detonation associated with a velocity of the burnt gas relaxing to its CJ value in the planar case $\mu_b(\tau) \to 0^+$. This problem can be solved in the limit (16) when the supporting piston is suddenly arrested [3]. For a stable CJ detonation ($b < b_c$), the end of the relaxation towards the marginal regime is described by

$$\mu_b(\tau) \to 0^+ : \qquad 2y(\tau) = \int_{-\infty}^{0} g(\xi)\, y(\tau + \bar{\zeta}(\xi))\mathrm{d}\xi + \epsilon\mu_b^2(\tau - |\bar{\zeta}_b|)/2 \tag{38}$$

the square in the forcing term being the signature of the marginality of the CJ wave. Using $\int_{-\infty}^{0} g(\xi)\,\mathrm{d}\xi = 1$ the quasi-steady approximation of (38) $\dot{\alpha}_\tau(\tau - |\bar{\zeta}_b|) \approx \dot{\alpha}_\tau(\tau)$ yields,

$$y \approx b\mu_b^2(\tau)/2 \quad \Leftrightarrow \quad \dot{\alpha}_\tau(\tau) \approx \mu_b^2(\tau)/2 \tag{39}$$

recovering the classical quadratic relation between the propagation velocity of slightly overdriven detonation and the velocity of the burnt gas in the limit $\mu_b \ll 1$. The decay to the CJ regime of a marginally stable or unstable detonation ($b \approx b_c$) is described by a nonlinear equation [3],

$$\kappa = 0, \quad \mu_b(\tau) \to 0^+ : \qquad 2y(\tau) = \int_{-\infty}^{0} G\Big(\xi, y(\tau + \bar{\zeta}(\xi))\Big)\mathrm{d}\xi + b\mu_b^2(\tau)/2 \tag{40}$$

written for a forcing term evolving slowly, $\mu_b^{-1}\mathrm{d}\mu_b/\mathrm{d}\tau \ll |\bar{\zeta}_b|^{-1}$ so that $\mu_b^2(\tau - |\bar{\zeta}_b|) \to \mu_b^2(\tau)$. For stable detonations, the quasi-steady relaxation (39) is effectively observed while nonlinear oscillations of $y(\tau)$ with a period of oscillation of order unity are superimposed to the quasi-steady relaxation for marginally unstable detonations.

It is worth mentioning that an integral equation similar to (35), but with a different time lag, was obtained previously [10] in the opposite limit of small heat release, namely for strongly overdriven detonations and large heat release $M_{0_{CJ}}^2 \gg 1$. In this limit, in contrast to what is said below (24) in the limit (16), the compressible modes $\mathcal{C}_+$ and $\mathcal{C}_-$ propagate faster than the entropy wave. The integral equation is the same as (35) with the difference that the delay is now associated with the downstream running entropy wave, the loop being closed quasi-instantaneously by the upstream running $\mathcal{C}_+$. A description of real detonations is obtained with a good quantitative accuracy by (35) into which the sum of the two delays (of the entropy wave and of the compressible mode $\mathcal{C}_+$) is introduced, the role of the compressible mode $\mathcal{C}_-$ being limited to relate the fluctuations of pressure and velocity as is indicated below (25). This indicates how useful are asymptotic analyses to describe the dynamics of real detonations, at least qualitatively, even when they correspond to limiting values of the parameters that are not well representative of real situations.

6. Asymptotic analysis of the decay to the CJ regime in spherical geometry

6.1. Condition at the exit of the reaction zone

The first difficulty mentioned at the end of § 3.2 concerns the evolution of the flow at the exit of the reaction zone. When approaching the CJ regime, this flow is quasi-transonic in real detonations. Following the pioneering works concerning pure shock waves, the problem is easily solved in planar geometry when detonations are considered as discontinuities. Thanks to the marginal character of the CJ regime, the perturbations of the flow of burnt gas, introduced by the entropy wave and the $\mathcal{C}_-$ mode, are negligible. The entropy being not disturbed, the rarefaction wave in the burnt gas (inert flow) is simply the continuation of the centred rarefaction wave (isentropic self-similar solution) developing as soon as the piston is suddenly arrested. This is also true when the response of the inner structure of the detonation is taken into account [3], yielding in the limit (16), $\mu_b(\tau) = \alpha(\tau)/\tau$, so that the 1967 relaxation law $\mathcal{D} - \mathcal{D}_{0_{CJ}} \propto 1/t^2$ is recovered when the response of the inner structure is neglected, $\dot{\alpha}_\tau \approx (\alpha/\tau)^2/2$.

In spherical geometry, retaining the term $-2u/r$ in (6), the decay is different. Under the approximation of a detonation considered as a discontinuity, there is no curvature-induced modification of the inner structure. However, the divergence of the flow $-2u/r$ plays an important role; in contrast to the planar case, the CJ velocity is reached at a finite time and at a finite radius. In an enlightening paper, A. Liñan et al. (2012) [11] deciphered the transition between two self-similar solutions, namely the Sedov–Taylor solution to a strong non-reactive blast wave and the Zeldovich (1942)–Taylor (1950) solution to a spherical CJ detonation. They also showed that, thanks to the transonic character of the burnt gas flow at the detonation front, the final stage of the decay is a local phenomenon. This can also be viewed on (19) at the exit of the reaction zone $w = 0$ for $\mu \ll 1$ and $\dot{\alpha}_\tau \ll 1$,

$$\mathrm{d}\mu_b(\tau)/\mathrm{d}\tau = -\kappa(\tau) \tag{41}$$

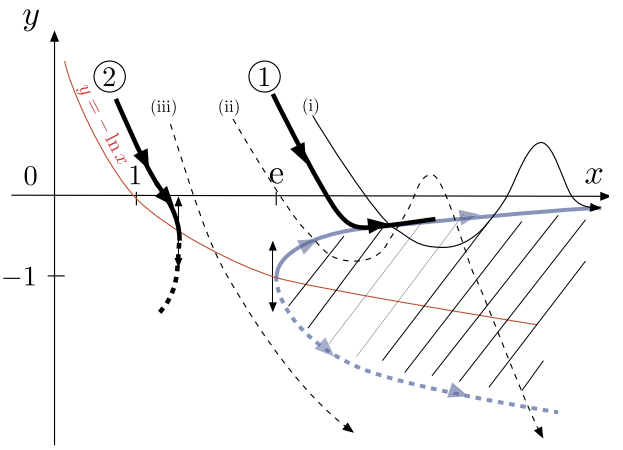

Fig. 2. Sketch of the trajectories in the phase space (y–x) "*propagation velocity–radius of the lead shock*". The boundary of the dashed region represents the spherical CJ waves (45) whose inner structure is in a steady state, the blue solid line being the upper branch. The black solid lines are the quasi-steady trajectories (48). Line 1 represents a success of the initiation process while line 2 is a failure. Typical results of direct numerical simulations [5–7] for stable or marginally unstable detonations are sketched by the thin dark lines. Line (i) is a success of the initiation process while lines (ii) and (iii) are failures. The difference between the numerical results and lines 1 and 2 illustrates the unsteadiness of the inner structure.

This relation between the time derivative of the flow velocity and the radius is the same as the one obtained by A. Liñan et al. (2012) [11] for a detonation front of zero thickness (no modification to the inner structure) and in a limit opposite to (16), namely for a large propagation Mach number $M_{\mathrm{o_{CJ}}} \gg 1$.

As mentioned in §2.2, small modifications to the inner structure of a curved detonation have a drastic effect if the induction is highly sensitive to temperature variations. As a result, initiation of a CJ detonation becomes a critical phenomenon; depending on the initial conditions, success or failure of the initiation process is produced. This was clearly pointed out in the limit $M_{\mathrm{o_{CJ}}} \gg 1$ using the square-wave model of detonation when unsteadiness in the inner structure is neglected, retaining only the geometrical modifications due to the curvature of the detonation wave [5]. Here, the purpose is to take into account the unsteady effects that are expected to be essential at the critical condition, as is shown by the direct numerical simulations sketched in Fig. 2. This can be achieved analytically for any chemical kinetics in the limit of small heat release by investigating the solution to (19)–(20) using (27) and the boundary condition (41) at the exit of the reaction zone. We will just outline the analysis; the details are given in a companion article [4]. It is worth revisiting first the spherical CJ waves when the inner structure is assumed to be in a steady state.

6.2. Spherical CJ waves in a steady state. CJ peninsula

Consider the steady version of (19) for $\kappa \neq 0$, neglecting the unsteady term $\partial\mu/\partial\tau$, and look for the solution satisfying the boundary conditions (20)–(26) with, according to (29), $\xi_{\mathrm{b}} = -\mathrm{e}^{-b\dot{\alpha}_{\tau_{\mathrm{CJ}}}}$. The steady-state solutions will be denoted with an overbar. When the parameter b is sufficiently large, the velocity of the CJ spherical velocity in steady state, expressed in terms of the curvature, $\bar{\dot{\alpha}}_{\tau_{\mathrm{CJ}}}(\kappa)$, presents a turning point and take the form of a peninsula in the phase space velocity–radius, see Fig. 2. The steady planar CJ wave $\mu_{\mathrm{o_{CJ}}}(\xi) = \sqrt{\int_{-1}^{\xi} \omega_{\mathrm{o_{CJ}}}(\xi')\mathrm{d}\xi'}$ in (31) is solution to (19) for $\kappa = 0$ and $\partial/\partial\tau = 0$. Anticipating that the turning point ($\kappa = \kappa^*$) corresponds to κ^* of order $1/b$ in the limit $b \gg 1$, the unknown μ in front of κ in the right-hand side of (19) can be replaced by $\mu_{o\mathrm{CJ}}(\xi)$ near the turning point,

$$b \gg 1: \qquad \kappa^* = O(1/b); \qquad \kappa/\kappa^* = O(1) \quad \Rightarrow \quad \mu\,\kappa \to \mu_{\mathrm{o_{CJ}}}\,\kappa \tag{42}$$

Integrating the so-modified version of (19) from the end of the reaction $\xi = -\mathrm{e}^{-b\bar{\dot{\alpha}}_{\tau_{\mathrm{CJ}}}}$ to the Neumann state $\xi = 0$ then yields the solution in the form propagation velocity versus radius $\bar{\dot{\alpha}}_{\tau_{\mathrm{CJ}}}(\kappa)$. Introducing the parameter $\lambda \in [1, 2]$,

$$\lambda \equiv 1 + \int_{-1}^{0} \mu_{\mathrm{o_{CJ}}}(\xi)\mathrm{d}\xi \tag{43}$$

with the reduced velocity and radius of the shock front, y and x, of order unity near the turning point,

$$b \gg 1: \quad y \equiv b\dot{\alpha}_\tau = O(1), \quad \bar{y}_{\mathrm{CJ}} \equiv (b\bar{\dot{\alpha}}_{\tau_{\mathrm{CJ}}}) = O(1), \quad 1/x \equiv (b\kappa)\lambda = O(1) \tag{44}$$

the equation of the peninsula in the phase space velocity–radius y–x for the spherical CJ detonations whose inner structure is in steady state $\bar{y}_{\mathrm{CJ}}(x)$ takes the form

$$b \gg 1: \quad \bar{y}_{CJ} + \frac{1}{x} e^{-\bar{y}_{CJ}} = 0 \tag{45}$$

There is no solution for a radius smaller than a critical value $x < x^*$, the coordinates of the turning point being ($x^* = e$, $y^* = -1$). The propagation velocity of curved CJ waves is smaller than that of the planar CJ wave, $\bar{y}_{CJ} < y_{o_{CJ}} = 0$ ($\mathcal{D} < \mathcal{D}_{o_{CJ}}$), and the solutions on the upper branch of the peninsula go to the planar CJ solution $\mathcal{D} = \mathcal{D}_{o_{CJ}}$ when the radius increases. The lower branch corresponds to a failure of the initiation process, since the difference $(\mathcal{D}_{o_{CJ}} - \mathcal{D}) > 0$ increases with the radius, see Fig. 2.

6.3. Quasi-steady trajectories near the CJ peninsula

According to the propagation velocity of the lead shock $\mathcal{D} = dr_f/dt$ with the relations (17)–(18), (25) and (41)–(44), the velocity of the flow at the exit of the reaction zone can be related to the radius of the lead shock r_f, yielding the expressions $\mu_b(\tau)$ and/or $\mu_b(x)$ in the phase space velocity–radius, the reduced radius x being a linear function of the time near the CJ peninsula,

$$dx/d\tau = 1/(b\lambda), \quad x/x_i = 1 + (\tau - \tau_i)/(\lambda b x_i), \quad d\mu_b/d\tau = -1/(b\lambda x), \quad \mu_b(x) = \mu_{bi} - \ln(x/x_i) \tag{46}$$

the subscript i denoting an initial condition. Consider quasi-steady overdriven detonations approaching the CJ regime. In planar geometry and in the limit $b \gg 1$, $\mu_b = O(1/\sqrt{b})$, $\bar{y} = O(1)$, the velocity profile of the quasi-steady inner structure of a weakly-overdriven detonation (31) takes the form

$$b \gg 1, \ \kappa = 0: \quad \bar{\mu}(\xi) = \sqrt{\mu_b^2 + \mu_{o_{CJ}}^2 (\xi\, e^{b\mu_b^2/2})} + O(1/b), \qquad \bar{\mu}(\xi) = \mu_{o_{CJ}}(\xi\, e^{b\mu_b^2/2}) + O(1/\sqrt{b}) \tag{47}$$

the relaxation of the propagation velocity to its CJ value being given in (39). The quasi-steady trajectories of spherical detonations $\bar{y}(x)$, are obtained from the solutions to the steady version of the partial differential equation (19), modified as indicated in (42), by using the boundary conditions (20) with (46). The so-obtained trajectories $\bar{y}(x)$ are solutions to the nonlinear equation

$$b \gg 1: \qquad \bar{y} + \frac{1}{x} e^{-\bar{y}} = m^2(x) \quad \text{where} \quad m \equiv \sqrt{b}\, \mu_b/\sqrt{2} = O(1) \tag{48}$$

The decreasing function $m(x)$, given by (46), depends on the initial condition. The trajectories $\bar{y}(x)$, solution to (48), show two different behaviours depending on the initial conditions $(x_i, \bar{y}_i)$ which corresponds to a negative slope $d\bar{y}/dx|_{x=x_i} < 0$ and a positive value of m, $m_i \equiv m(x_i) > 0$. For initial conditions such that the trajectory $\bar{y}(x)$ goes down to $y = 0$ for a radius larger than the critical radius $x > x^* = e$, the upper branch of the CJ peninsula ($m = 0$) is reached tangentially, in a way similar to the planar case studied in [11] when the modification of the inner structure is neglected, $\mathcal{D} \to \mathcal{D}_{o_{CJ}}$. If not, the slope of the trajectories $d\bar{y}_{CJ}/dx$ goes to $-\infty$ at $y = -\ln x$ with $x < x^*$, see Fig. 2. The validity of the analysis stops there. The trajectory is expected to go below the CJ peninsula in agreement with the real initiation process, a successful initiation being produced only if the energy that is deposited is sufficiently large for making the trajectories crossing the CJ peninsula, as conjectured in [5].

Unfortunately, the quasi-steady analysis is not valid. In the limit $b \gg 1$, the contribution of the unsteady term in (19), evaluated from (46)–(48), is in fact larger than the small curvature term,

$$\int_{-e^{-\bar{y}_{CJ}}}^{0} (\partial\bar{\mu}/\partial\tau)\, d\xi = -(\lambda - 1)\frac{d\bar{y}}{d\tau} e^{-\bar{y}_{CJ}} \quad \text{where} \quad \frac{d\bar{y}}{d\tau} = \frac{d\bar{y}}{dx}\frac{dx}{d\tau} = O(m/\sqrt{b}) \tag{49}$$

so that the integral is of order $(\lambda - 1)/\sqrt{b}$, larger than the curvature term in (19), which is, according to (42), of order $1/b$. Therefore the asymptotic analysis should retain the unsteadiness.

6.4. Integral equation for the dynamics near the CJ peninsula

In the context of the direct initiation process, the decay of spherical detonations, taking into account the unsteadiness of the inner structure, can be studied in the limits (16) and (42) by considering the ordering

$$b \gg 1: \qquad (\lambda - 1)/\lambda = h/\sqrt{2b} \quad \text{with} \quad h = O(1) \tag{50}$$

so that the effect of unsteadiness is, according to (49), of the same order of magnitude as the one of curvature $\kappa = O(1/b)$. This is a good approximation for an ordinary distribution of the reaction rate for which $\lambda \approx 1.5$ when $b = 10$, yielding $h \approx 1.5$. The attention is focused upon the regimes that are close to the CJ peninsula, so that the velocity profile $\mu(\xi, \tau)$ is close to the profile $\bar{\mu}(\xi, \tau)$ of planar overdriven detonations decaying in a quasi-steady state to the CJ regime. According to

(47), the ξ-dependence of this reference unsteady profile is that of the planar CJ wave rescaled by the unsteady induction length, $\overline{\mu}(\xi,\tau)=\overline{\mu}_o(\xi\,\mathrm{e}^{m^2(\tau)},\,\tau)$, $\overline{\mu}_o(\xi,\tau)=\sqrt{\sqrt{2}m(\tau)/\sqrt{b}+\mu^2_{\mathrm{o_{CJ}}}(\xi)}$, where $m(\tau)=O(1)$ is a linear function of time, see (46) and (48),

$$m=m_i-\sqrt{b/2}\ln(x/x_i)=m_i-\sqrt{b/2}\ln[1+(\tau-\tau_i)/bx_i]\approx m_i-(\tau-\tau_i)/(x_i\sqrt{2b})\geqslant 0 \tag{51}$$

Following a method similar to the analyses discussed above, an integral equation is obtained for $y(\tau)$ involving the unsteady time delay

$$\zeta(\xi,\tau)\equiv-\int_{\xi}^{0}\frac{\mathrm{d}\xi'}{\overline{\mu}(\xi',\tau)}=-\,\mathrm{e}^{-m^2(\tau)}\int_{\xi\,\mathrm{e}^{m^2(\tau)}}^{0}\frac{\mathrm{d}\xi'}{\overline{\mu}_{\mathrm{o}}(\xi',\tau)}<0,\qquad |\zeta(\xi,\tau)|<\infty \tag{52}$$

From a given initial condition $m_i=O(1)$, $m_i>0$, according to (51), the time taken by the quasi-steady overdriven detonation to reach the CJ regime ($m=0$) is of order $\sqrt{b}$, $(\tau-\tau_i)/\tau_i=O(\sqrt{b})$, so that the flow velocity at the exit of the reaction zone evolves slowly at the scale of the response of the inner structure, $\delta\tau/\tau=O(1)$. For saving the notations, we use the notation $m(\tau)$, keeping in mind that $m(\tau)$ varies of order unity for $(\tau-\tau_i)/\tau_i=O(\sqrt{b})$. However, the delay $|\zeta(\xi,\tau)|$ increases when approaching the end of the reaction zone, where it becomes larger than unity and diverge at the CJ regime ($m\to 0^+$) like $\sqrt{b/m}$, see [4], so that a quasi-steady state assumption cannot be valid. Skipping the technical details of the analysis presented in [4], the integral equation for the propagation velocity $y(\tau)$, as is obtained by the asymptotic analysis in the limits (16) and $b\gg 1$, is a composite expression of (40) and (48) plus additional unsteady terms:

$$\begin{aligned}y(\tau)+\frac{1}{x(\tau)}\mathrm{e}^{-y(\tau)}=m^2(\tau)&+\int_{-\infty}^{0}W\Big(\xi,y(\tau+\zeta)\Big)\mathrm{d}\xi\\&+\int_{-\infty}^{0}\mu'_{\mathrm{o_{CJ}}}(\xi\mathrm{e}^{m^2(\tau)})[y(\tau+\zeta)-y(\tau)]\mathrm{e}^{m^2(\tau)}\mathrm{d}\xi-\frac{h}{x(\tau)}\mathrm{e}^{-m^2(\tau)}m(\tau)\end{aligned} \tag{53}$$

where $W(\xi,\,y)$ is given in (36) and the notation $\mu'_{\mathrm{o_{CJ}}}(\xi)\equiv \mathrm{d}\mu_{\mathrm{o_{CJ}}}(\xi)/\mathrm{d}\xi$ has been used. The two integral terms on the right-hand side of (53) come from the response of the inner structure similar. Neglecting the curvature and the time dependence of m, the planar case, (35)–(36) and (40), is recovered. The last term on the right-hand side is the unsteady effect (49) coming from the zeroth-order solution $\mu_{\mathrm{o_{CJ}}}(\xi\mathrm{e}^{m^2(\tau)})$ using $\mathrm{d}m^2/\mathrm{d}\tau=b\mu_{\mathrm{b}}\mathrm{d}\mu_{\mathrm{b}}/\mathrm{d}\tau=-\sqrt{2b}\,m/\lambda x$, see (46). The curved CJ waves $m=0$ are now unsteady and differ from the CJ peninsula (45) because of unsteadiness of the inner structure, the CJ peninsula being recovered only when the time delay is neglected $y(\tau+\zeta)\to y(\tau)$ by using (36). The quasi-steady trajectories $\overline{y}(x)$, obtained from (53), $\overline{y}(x)+\mathrm{e}^{-\overline{y}(x)}/x=m^2(x)-h\mathrm{e}^{-m^2(x)}m(x)/x$, differ from (48) by the last term, which is the unsteady effect identified in (49). Each trajectory $\overline{y}(x)$ is associated with its initial condition $(y_i,\,x_i)$ related to m_i by the relation $y_i+\mathrm{e}^{-y_i}/x_i=m_i^2-h\mathrm{e}^{-m_i^2}m_i/x_i$.

7. Discussion and perspective

For a typical distribution $w_{\mathrm{o_{CJ}}}(\xi)$, the value of the parameter b at the instability threshold is of order unity, $b_{\mathrm{c}}=O(1)$, so that planar detonations are strongly unstable in the limit $b\gg 1$. In order to extend the analysis to marginally stable and/or unstable detonations ($b\approx b_{\mathrm{c}}$), the parameter b appearing in the final result in the expression (36) of $W(\xi,\,y)$ with $\int_{-\infty}^{0}W(\xi,\,y)\mathrm{d}\xi=0\ \forall b$, should be considered of order unity. This is justified by noticing that, in real detonations ($M^2_{\mathrm{o_{CJ}}}\gg 1$), the coefficient of proportionality between the critical radius r_f^* and the detonation thickness $d_{\mathrm{o_{CJ}}}$ is larger than the parameter controlling the dynamics through the thermal sensitivity of the induction length, see [5], while the two parameters become identical in the limit of small heat release (16) used here to solve analytically the dynamics of the inner structure, see (44)–(45).

Near the instability threshold ($b\approx b_{\mathrm{c}}$), the complex dynamics near criticality ($r_{\mathrm{f}}(t)\approx r_{\mathrm{f}}^*$, $x^*=\mathrm{e}$), which is sketched in Fig. 2, is well reproduced by the numerical solutions to (53) for various initial conditions $(x_i,\,y_i)$ assumed to be in quasi-steady state, $y\geqslant y_i: y\approx\overline{y}(x)$, see [4]. The unsteady effect is reinforced when approaching the CJ regime by a long-range time delay. The relative importance of unsteadiness and curvature effect upon the critical dynamics can be carefully analyzed from (53). The critical dynamics cannot be recovered when suppressing one of the two mechanisms in (53). In that respect, both are essential, in contrast to the point of view expressed in [7] "*the primary failure mechanism is found to be unsteadiness*". Moreover, the critical radius is not very different from r_{f}^* predicted in (44)–(45) using a steady-state approximation ($x^*=\mathrm{e}$).

An extension of the asymptotic analysis to a more realistic limit than (16), namely for a large propagation Mach number, $M^2_{\mathrm{o_{CJ}}}\gg 1$, is in process by the method mentioned at the end of § 5.2.

Acknowledgements

Amable Liñan and Yves Pomeau are acknowledged for stimulating discussions. Partial financial support is provided by the “Agence nationale de la recherche” (contract No. ANR-18-CE05-0030).

References

[1] P. Clavin, Nonlinear dynamics of shocks and detonation waves in gases, Combust. Sci. Technol. 189 (2017) 747–775.
[2] P. Clavin, G. Searby, Combustion Waves and Fronts in Flows, Cambridge University Press, 2016.
[3] P. Clavin, B. Denet, Decay of plane detonation waves to the self-propagating Chapman–Jouguet regime, J. Fluid Mech. 845 (2018) 170–202.
[4] P. Clavin, B. Denet, Asymptotic analysis of direct initiation of gaseous detonation, J. Fluid Mech. (2019), submitted for publication.
[5] L. He, P. Clavin, On the direct initiation of gaseous detonations by an energy source, J. Fluid Mech. 277 (1994) 227–248.
[6] L. He, Theoretical determination of the critical conditions for the direct initiation of detonation in hydrogen-oxygen mixtures, Combust. Flame 104 (1996) 401–418.
[7] C.A. Eckert, J.J. Quirk, J.E. Shepherd, The role of unsteadiness in direct initiation of gaseous detonation, J. Fluid Mech. 421 (2000) 147–183.
[8] P. Clavin, F.A. Williams, Dynamics of planar gaseous detonations near Chapman–Jouguet conditions for small heat release, Combust. Theory Model. 6 (2002) 127–139.
[9] P. Clavin, F.A. Williams, Multidimensional stability analysis of gaseous detonations near Chapman–Jouguet conditions for small heat release, J. Fluid Mech. 624 (2009) 125–150.
[10] P. Clavin, L. He, Stability and nonlinear dynamics of one-dimensional overdriven detonations in gases, J. Fluid Mech. 306 (1996) 353–378.
[11] A. Liñan, V. Kurdyumov, A. Sanchez, Initiation of reacting blast waves by external energy sources, C. R. Mecanique 340 (2012) 829–844.